

This discussion paper is/has been under review for the journal Atmospheric Chemistry and Physics (ACP). Please refer to the corresponding final paper in ACP if available.

A Tropical West Pacific OH minimum and implications for stratospheric composition

M. Rex¹, I. Wohltmann¹, T. Ridder², R. Lehmann¹, K. Rosenlof³, P. Wennberg⁴,
D. Weisenstein⁵, J. Notholt², K. Krüger^{6,*}, V. Mohr⁶, and S. Tegtmeier⁶

¹Alfred Wegener Institute for Polar and Marine Research, Potsdam, Germany

²Institute of Environmental Physics, University of Bremen, Bremen, Germany

³NOAA ESRL Chemical Sciences Division, Boulder, CO, USA

⁴California Institute of Technology, Pasadena, CA, USA

⁵Atmospheric and Environmental Research, Inc., Lexington, MA, USA

⁶Helmholtz Centre for Ocean Research Kiel (GEOMAR), Kiel, Germany

* now at: University of Oslo, Oslo, Norway

Received: 16 October 2013 – Accepted: 18 October 2013 – Published: 5 November 2013

Correspondence to: M. Rex (markus.rex@awi.de)

Published by Copernicus Publications on behalf of the European Geosciences Union.

Title Page

Abstract

Introduction

Conclusions

References

Tables

Figures

◀

▶

◀

▶

Back

Close

Full Screen / Esc

Printer-friendly Version

Interactive Discussion



Abstract

Hundreds of biogenic and anthropogenic chemical species are emitted into the atmosphere. Most break down efficiently by reaction with OH and do not reach the stratosphere. Here we show the existence of pronounced minima in the tropospheric columns of ozone and OH over the West Pacific, the main source region for stratospheric air. We show that this amplifies the impact of surface emissions on the stratospheric composition. Specifically, emissions of biogenic halogenated species from natural sources and from kelp and seaweed farming can have a larger effect on stratospheric ozone depletion. Increasing anthropogenic emissions of SO₂ in South East Asia or from minor volcanic eruptions can play a larger role for the stratospheric aerosol budget, a key element for explaining the recently observed decrease in global warming rates (Solomon et al., 2011).

1 Introduction

The overall composition of the stratosphere is mainly determined by species that ascend from the surface through the troposphere and tropopause into the stratosphere. Reaction with OH radicals in the troposphere convert most molecules into soluble breakdown products, which are removed by rainout or deposition on ice that forms near the temperature minimum at the tropopause (WMO, 2011). Hence, the presence of OH in the troposphere shields the stratosphere from most surface emissions and is particularly relevant for compounds that do not photolyse efficiently.

Much of our understanding of transport of short lived species into the stratosphere is based on studies that assume fixed uniform lifetimes (WMO, 2011, cf. chapter 1.3.2). But the degree of temporal and spatial variability of tropospheric OH is subject of ongoing debate (Manning et al., 2005; Montzka et al., 2011; Hanisco et al., 2001; Rohrer and Berresheim, 2006). It is key not only for the supply of chemical species to the stratosphere but also for the atmospheric lifetimes of many greenhouse gases and

A Tropical West Pacific OH minimum

M. Rex et al.

Title Page

Abstract

Introduction

Conclusions

References

Tables

Figures

◀

▶

◀

▶

Back

Close

Full Screen / Esc

Printer-friendly Version

Interactive Discussion



for deriving their source terms from measurements of their atmospheric abundances (Manning et al., 2005). A major source of OH in clean tropical air is formation through:



5 This couples the OH concentration and hence the oxidizing capacity of tropospheric air closely to the ozone concentration (Levy II, 1971; Jaeglé et al., 2001). The OH concentration further depends on the concentration of NO, which controls the conversion of HO₂ into OH:



10 2 Measurements and chemistry of OH and ozone

The Western Pacific warm pool, where sea surface temperatures are highest globally, is the major source region for stratospheric air (Newell and Gould-Stewart, 1981; Fueglistaler et al., 2004). Information on tropospheric ozone profiles from there has been very limited so far. Measurements from the south east edge of the warm pool
15 in 1993 (Kley et al., 1996) and individual profiles from the station Samoa considerably further south east (Solomon et al., 2005) showed extremely low ozone in the marine boundary layer and at tropopause levels. A reduced oxidizing capacity of the tropopause region above the Central Pacific was derived from these data (Kley et al., 1996). However, these measurements showed significant amounts of ozone in most of
20 the free troposphere. Moreover, these data are not from the key region of troposphere to stratosphere transport.

Figure 1 shows tropospheric ozone mixing ratios determined by sonde measurements during the TransBrom cruise with the Research Vessel (RV) Sonne roughly along 140–150° E in October 2009 (Krüger and Quack, 2013). In all six profiles in the central
25 part of the warm pool between 15° N and 10° S ozone was at or below the detection

A Tropical West Pacific OH minimum

M. Rex et al.

Title Page

Abstract

Introduction

Conclusions

References

Tables

Figures

◀

▶

◀

▶

Back

Close

Full Screen / Esc

Printer-friendly Version

Interactive Discussion



limit throughout the troposphere (see Appendix for discussion of the detection limit and robustness of the measurements).

Reactions (R1) and (R2) provide an efficient loss mechanism for ozone (Liu et al., 1983). The efficiency is a function of actinic fluxes at $\lambda < 340$ nm (in clear sky conditions mostly determined by overhead ozone and solar zenith angle) and concentration of water vapor, with higher air temperatures corresponding to higher water concentrations and faster ozone loss. This favors ozone loss over the westernmost tropical Pacific, where marine boundary layer air temperature is highest and overhead ozone lowest. Odd oxygen (O_3+O) lifetimes (which determine the effective lifetime of ozone) drop to 4 days under these conditions (lifetime calculation in Appendix).

The odd oxygen lifetime increases steeply with altitude due to decreasing temperature, leading to lower water vapor. But the high sea surface temperatures also favour strong convective activity in the tropical West Pacific. Loss in the boundary layer combined with convectively driven vertical mixing is the most likely explanation for the near complete loss of ozone throughout the troposphere there.

Due to the general low and mid-tropospheric advection from the east across the vast Pacific, air above the tropical westernmost Pacific has been in a clean, warm and humid environment for a long time and loss of odd oxygen and of ozone precursors like NO_x ($= NO + NO_2$, NO_x is lost by conversion into HNO_3 followed by washout) proceeded longer than elsewhere in the tropics. In situ-measurements in the tropopause region close to Hawaii during STRAT, a campaign with the ER-2 high altitude research aircraft, include O_3 , NO and OH (Fig. 2). A patch of air originating from the convective outflow area in the West Pacific was probed, which was transported to Hawaii by tropopause level advection (red circle in Fig. 2, corresponding air mass trajectory in the Appendix). This air was characterized by extremely low ozone and NO . Low NO further reduces OH concentrations by Reaction (R3). OH concentrations in this air mass are up to a factor of four smaller than those observed in the compact OH vs. solar zenith angle relation reported by Hanisco et al. (2001) for similar altitudes.

A Tropical West Pacific OH minimum

M. Rex et al.

Title Page

Abstract

Introduction

Conclusions

References

Tables

Figures

◀

▶

◀

▶

Back

Close

Full Screen / Esc

Printer-friendly Version

Interactive Discussion



**A Tropical West
Pacific OH minimum**

M. Rex et al.

[Title Page](#)[Abstract](#)[Introduction](#)[Conclusions](#)[References](#)[Tables](#)[Figures](#)[◀](#)[▶](#)[◀](#)[▶](#)[Back](#)[Close](#)[Full Screen / Esc](#)[Printer-friendly Version](#)[Interactive Discussion](#)

The ship and aircraft measurements provide local snapshots of atmospheric conditions. We have used measurements of the satellite borne Tropospheric Emission Spectrometer (TES) and the GEOS-Chem tropospheric Chemistry Transport Model (CTM; cf. Ridder et al. (2012) for details of the model runs) to assess the geographical extent and the persistence of the tropospheric ozone and OH minima.

Figure 3a shows the monthly mean tropospheric ozone column for October 2009 from TES. The data are in good agreement with the sonde data (shown as dots) and combined OMI/MLS satellite data (Ziemke et al., 2006; Joiner et al., 2009), confirming the pronounced tropospheric ozone minimum above the warm pool. The satellite data show that this feature is persistent, present during all years of TES measurements and mostly year round (see Appendix).

3 Model calculations of OH and air mass trajectories

Ridder et al. (2012) showed that GEOS-Chem reproduces ozone and CO observations very well and the main features are robust among a wide range of tropospheric CTMs (Stevenson et al., 2006). Figure 3b, c show the modeled distribution of the tropospheric ozone and OH column in the tropics for the first half of October 2009. Pronounced minima in the tropospheric columns of ozone and OH are present over the westernmost tropical Pacific. For further discussion we define an “OH minimum area” (125° E to 140° E) and an “outside minimum area” (80° W to 100° E) in the inner tropics (10° S to 10° N). In the “OH minimum area” the minimum ozone column is only 28% and the minimum OH column is only 22% of the respective average column for the “outside minimum area”.

This has a large impact on lifetimes of chemical species in that region. Figure 3f, g show CH₂Br₂ and gas phase SO₂ lifetimes as examples of key species at 500 hPa inside and outside of the “OH minimum area”.

Removal of species depends on the oxidation efficiency along the air mass trajectories between the boundary layer and the tropopause. Near the tropical tropopause air

masses go through their temperature minimum, the Lagrangian Cold Point (LCP), encounter their last contact with condensed water and the last removal of soluble species by deposition takes place (Fueglistaler et al., 2004). Any later breakdown of species can only change the stratospheric balance between species but not the total budgets of e.g. halogens or sulfur.

Most air masses reach their LCP above the West Pacific (Fueglistaler et al., 2004; Bonazzola and Haynes, 2004; Krüger et al., 2008). We used the Lagrangian chemical transport model ATLAS (Wohltmann and Rex, 2009; Wohltmann et al., 2010) to determine the area in which air masses pass through the troposphere between their last contact with the boundary layer and the LCP (Fig. 3d). This “tropospheric transit region” correlates with the tropospheric ozone and OH minimum areas discussed above (Fig. 3a–c). This correlation results in a large impact of the OH minimum on the global scale, despite the relatively small size of the minimum: combining the transport calculations from ATLAS with the chemical fields from GEOS-Chem shows that the average OH concentration for all air masses that ascend into the stratosphere globally (during transport from the boundary layer to the LCP) is only 57 % of the average OH in the “outside minimum” area.

The transit time through the troposphere varies between individual air masses (Fig. 3h) and its distribution overlaps the chemical lifetimes of important species like dibromomethane (CH_2Br_2) and sulfur dioxide (SO_2). Hence the fraction of these species that reach the LCP is sensitive to the OH concentrations. Figure 4a shows that for “outside minimum area” conditions only 30 % of the air masses preserve more than 80 % of the dibromomethane present in the boundary layer, compared to 68 % for “OH minimum area” conditions.

4 Discussion and conclusions

Short lived halogenated species are believed to contribute to the stratospheric halogen budget and to amplify polar ozone loss (WMO, 2011). These species are produced

A Tropical West Pacific OH minimum

M. Rex et al.

Title Page

Abstract

Introduction

Conclusions

References

Tables

Figures

◀

▶

◀

▶

Back

Close

Full Screen / Esc

Printer-friendly Version

Interactive Discussion



by biological activity in the oceans and increasing kelp and seaweed farming in South East Asia (Quack et al., 2004; Pyle et al., 2011), which has been proposed for carbon dioxide sequestration and is believed to contribute to increasing emissions (Martinez-Aviles et al., 2010). Our findings show that emissions from such activity are more likely to reach the stratosphere, especially because this area belongs to the main source area of stratospheric air (Fig. 3e). This calls for a critical assessment of the impact of these activities on the stratospheric halogen budget and ozone loss.

Furthermore, our findings suggest a larger impact of increasing anthropogenic emissions of SO₂ in South East Asia (Thomason and Peter, 2006) or of weak to moderate volcanic eruptions (Hofmann et al., 2009; Vernier et al., 2011) on the stratospheric sulfur and aerosol budget, a key element for stratospheric chemistry and for explaining the recently observed decrease in global warming rates (Solomon et al., 2011).

Figure 4b shows the impact of the OH minimum on the aerosol distribution derived from the AER aerosol model (Thomason and Peter, 2006; Weisenstein et al., 1997). For “OH minimum” conditions the aerosol surface area density in the upper free troposphere drops by up to 25% (due to less efficient conversion of SO₂ into sulfate), while that in the lowermost stratosphere increases by more than 5% (due to transport of more SO₂ into the stratosphere and conversion into sulfate at higher altitudes).

These calculations were carried out for background SO₂ fluxes, corresponding to less than 50 pptv of SO₂ in the tropical boundary layer. The impact in the stratosphere well above the tropopause is limited because of the large and mainly unchanged contribution of COS. But anthropogenic SO₂ emissions from South East Asia and from dense ship traffic in the Pacific can substantially enhance surface SO₂ levels above background conditions, such that their relative contribution to the stratospheric sulfur budget is larger. Our findings suggest that increasing SO₂ emissions from South East Asia (Thomason and Peter, 2006) contribute to aerosol formation in the upper tropical troposphere and lower stratosphere and may contribute to the long term increase in aerosol loading observed there (Solomon et al., 2011).

A Tropical West Pacific OH minimum

M. Rex et al.

Title Page

Abstract

Introduction

Conclusions

References

Tables

Figures

◀

▶

◀

▶

Back

Close

Full Screen / Esc

Printer-friendly Version

Interactive Discussion



**A Tropical West
Pacific OH minimum**

M. Rex et al.

[Title Page](#)[Abstract](#)[Introduction](#)[Conclusions](#)[References](#)[Tables](#)[Figures](#)[◀](#)[▶](#)[◀](#)[▶](#)[Back](#)[Close](#)[Full Screen / Esc](#)[Printer-friendly Version](#)[Interactive Discussion](#)

Compared to these background conditions the effect on stratospheric aerosol will be much more pronounced in the event of weak to moderate volcanic eruptions depositing much larger amounts of SO₂ into the upper troposphere from where it is transported into the stratosphere (Hofmann et al., 2009) and plays a much larger role for the stratospheric sulfur budget than under background conditions. The presence of the OH minimum facilitates the transport of SO₂ into the stratosphere if volcanic injection occurs into the troposphere of that region. Hence, such smaller eruptions, which often do not directly inject sulfur into the stratosphere, can be more relevant for climate.

The tropospheric OH minimum is also relevant for global lifetimes of those greenhouse gases predominantly lost by chemical breakdown in the troposphere. This is the case for most of the HCFCs. The local lifetime of these species (e.g. CH₃CCl₃) is inversely proportional to OH concentrations and hence a factor of 3.5 longer in the OH minimum area compared to outside minimum conditions. This significantly increases global lifetimes and hence the global warming potential of these species.

Appendix A

Ozonesonde measurements

Ozone soundings were carried out following standard operation procedures with sondes manufactured by EnSci Corporation attached to Graw DFM-97 radiosondes. The ozonesondes were stored and prepared in an air conditioned room at approximately 26 °C room temperature and 60 % relative humidity. During preparation at the ground no difference in the cell current could be detected between measurements of ambient air and measurements with an ozone filter attached to the sonde. Two different ozone destruction filters were attached to the ozonesonde for all six soundings between 15° N and 8° S. These ground measurements were repeated both outside and in the air conditioned room. The ozone destruction filters were always stored in the low relative humidity environment and one of them was never taken outside, making any

adverse effect of high humidity on the efficiency of the filters very unlikely. In the stratosphere all ozonesondes measured normal tropical ozone profiles. The signal from most ozonesondes could be received by the ground station during descent after the burst of the balloon and ozone readings returned to values below the detection limit of the sensor when the sensor reached the troposphere again.

During the standard preparation of an ozonesonde at the ground electrochemical (ECC) ozone sensors exhibit a significant background current. The time evolution of that background current during the balloon ascent is not known and recommendations how to correct for the background current range from assuming a constant background throughout the sounding (recommended in the operation manual from EnSci corporation) over assuming a falloff of the background current as a function of pressure (recommended in the operation manual from Vaisala) to assuming that the background current drops to zero soon after launch (Vernier et al., 2011). Figure A1 shows one example of an ozone profile from the inner tropics derived from the cell current based on all three assumptions. The real evolution of the background current is unknown at present, because it has never been measured during flight. Until such measurements are available for a wide range of meteorological conditions the unknown evolution of the background current contributes to the uncertainty of ECC ozonesonde measurements at very low ozone concentrations and actually defines the detection limit of such sensors. Once the cell current falls below the background current (that has been measured before launch) the measurement is compatible with zero ozone concentrations. For these portions of the profiles ozone concentrations that are calculated from the cell current directly without background current subtraction (i.e. assuming that the background current immediately disappears after launch) defines the upper limit for the ozone concentrations. Based on this and typical background currents, the detection limit of ECC ozonesonde sensors is around 15 ppbv in the upper free troposphere and at the tropopause. The figures in the paper show the results based on Vaisala's recommendation for a pressure dependent background current and the shading in Fig. 1 illustrates the detection limit for typical background currents. Figure A1 shows that for

A Tropical West Pacific OH minimum

M. Rex et al.

[Title Page](#)[Abstract](#)[Introduction](#)[Conclusions](#)[References](#)[Tables](#)[Figures](#)[◀](#)[▶](#)[◀](#)[▶](#)[Back](#)[Close](#)[Full Screen / Esc](#)[Printer-friendly Version](#)[Interactive Discussion](#)

20.37–22.19° N, 159° W a patch of air was sampled that originated from the ozone and OH minimum in the West Pacific. A 12 day backtrajectory of the center of that airmass is shown in Fig. A3.

Appendix C

5 Tropospheric Emission Sounder (TES)

Tropospheric ozone columns for Figs. 3a and A4 were calculated from all available Level 2 profile data (with the master quality flag set) by integrating the mixing ratios between the surface and 150 hPa. Monthly means were calculated by binning the satellite measurements of a particular month. Figure 3a shows monthly means for October 2009. Minor local differences to the sonde data shown in the plot are within the range of the day to day variations in ozone shown by TES. A complete geographical coverage cannot be obtained from daily TES measurements. Figure A4 shows monthly averaged data for January, April, July, and October for the years 2005–2009.

Appendix D

15 ATLAS model

ATLAS is a global Chemistry and Transport Model based on a Lagrangian (trajectory-based) transport and mixing scheme (Wohltmann and Rex, 2009; Wohltmann et al., 2010). Here we use the trajectory module of the model in a stand-alone mode. Trajectory calculations are driven by ECMWF ERA-Interim reanalysis data (Dee et al., 2011). The vertical coordinate of ATLAS is a hybrid pressure-potential temperature coordinate. Corresponding vertical winds are calculated from the vertical winds and the heating rates (including clouds) provided by ERA-Interim. For ten years (2002–2011)

A Tropical West Pacific OH minimum

M. Rex et al.

Title Page

Abstract

Introduction

Conclusions

References

Tables

Figures

◀

▶

◀

▶

Back

Close

Full Screen / Esc

Printer-friendly Version

Interactive Discussion



backward trajectory runs were started on 400 K between 30° S and 30° N on a 2° × 2° grid and run for 120 days. During these years interannual variability is limited and the results are presented as averages over all years. Time and location of the passages through the Lagrangian Cold Point (LCP) and the 800 hPa level (roughly corresponding to the top of the planetary boundary layer) were recorded for every trajectory. Figure 3d shows the density distribution function (trajectory air parcels per area) of all locations of the trajectory air parcels between their passage through 800 hPa and their individual LCPs, i.e. all positions in longitude and latitude at every 10 min time step between these passages, regardless of altitude. Figure 3e shows the density distribution function for the passages through 800 hPa.

Appendix E

Lifetime calculations

For the calculation of the lifetimes of CH₂Br₂ and SO₂ given in Fig. 3f, g the reactions of these species with OH and, in the case of CH₂Br₂, the photolysis were taken into account. Reaction rate constants from Sander et al. (2011) and daily-mean photolysis rates calculated by TUV (Tropospheric Ultraviolet–Visible Model, Madronich and Flocke, 1999) were used. The calculated lifetimes correspond to conditions at 500 hPa above the Equator on 1 October. OH concentrations were assumed to be 7×10^5 and 24×10^5 molecules cm⁻³, respectively. These values represent the minimum and maximum values determined by the GEOS-Chem model at 500 hPa above the Equator (near 135° E and 0° E, respectively). Under these conditions, the lifetime of CH₂Br₂ is determined almost completely by the reaction with OH, because the photolysis contributes less than 1 % to the CH₂Br₂ loss.

The odd oxygen lifetime was calculated from daily-mean odd oxygen loss rates determined by a chemical box model (reaction rate constants and photolysis as cited above) for near-surface conditions at the Equator under the assumption of 80 % rel-

ative humidity at 26°C. Under these conditions, the lifetime of odd oxygen is mainly determined by the loss reaction (R2).

The calculation of the breakdown of CH₂Br₂ for Fig. 4a was done with the same photochemical model. The box model was run along each trajectory between 800 hPa and the Lagrangian cold point and results were averaged over all trajectories. The percentage of the CH₂Br₂ reaching the stratosphere was determined by dividing the CH₂Br₂ mixing ratios at the LCP by those at 800 hPa. Temperatures along the trajectories were taken from the ERA-Interim reanalysis. Photolysis rates were calculated from the solar zenith angles on the trajectories and an overhead ozone value of 300 DU. OH was determined from the October GEOS-Chem field by averaging model results longitudinally over 125°E–140°E for the “OH hole” conditions and 80°W–100°E for the “outside hole” conditions to give 2-dimensional latitude-pressure fields. These values were interpolated on the trajectories.

Acknowledgements. This work was supported by the European Community within the SHIVA project (grant no. 226224). TransBrom was financed by the BMBF (grant no. 03G0731A). We thank Ru-Shan Gao (NOAA) for his contributions and sharing his data. Susan Tegtmeier and Viktoria Mohr were funded by the WGL project TransBrom. We thank ECMWF for providing ERA Interim data.

References

- Bonazzola, M. and Haynes, P. H.: A trajectory-based study of the tropical tropopause region, *J. Geophys. Res.*, 109, D20112, doi:10.1029/2003JD004356, 2004. 28874
- Dee, D. P., Uppala, S. M., Simmons, A. J., Berrisford, P., Poli, P., Kobayashi, S., Andrae, U., Balmaseda, M. A., Balsamo, G., Bauer, P., Bechtold, P., Beljaars, A. C. M., van de Berg, L., Bidlot, J., Bormann, N., Delsol, C., Dragani, R., Fuentes, M., Geer, A. J., Haimberger, L., Healy, S. B., Hersbach, H., Hólm, E. V., Isaksen, I., Kållberg, P., Köhler, M., Matricardi, M., McNally, A. P., Monge-Sanz, B. M., Morcrette, J.-J., Park, B.-K., Peubey, C., de Rosnay, P., Tavolato, C., Thépaut, J.-N., and Vitart, F.: The ERA-Interim reanalysis: configuration and

A Tropical West Pacific OH minimum

M. Rex et al.

Title Page

Abstract

Introduction

Conclusions

References

Tables

Figures

◀

▶

◀

▶

Back

Close

Full Screen / Esc

Printer-friendly Version

Interactive Discussion



A Tropical West Pacific OH minimum

M. Rex et al.

Title Page

Abstract

Introduction

Conclusions

References

Tables

Figures

◀

▶

◀

▶

Back

Close

Full Screen / Esc

Printer-friendly Version

Interactive Discussion



performance of the data assimilation system, Q. J. Roy. Meteorol. Soc., 137, 553–597, 2011. 28879

Fueglistaler, S., Wernli, H., and Peter, T.: Tropical troposphere-to-stratosphere transport inferred from trajectory calculations, J. Geophys. Res., 109, D03108, doi:10.1029/2003JD004069, 2004. 28871, 28874

Gao, R. S., Fahey, D. W., Salawitch, R. J., Lloyd, S. A., Anderson, D. E., DeMajistre, R., McElroy, C. T., Woodbridge, E. L., Wamsley, R. C., Donnelly, S. G., Del Negro, L. A., Proffitt, M. H., Stimpfle, R. M., Kohn, D. W., Kawa, S. R., Lait, L. R., Loewenstein, M., Podolske, J. R., Keim, E. R., Dye, J. E., Wilson, J. C., and Chan, K. R.: Partitioning of the reactive nitrogen reservoir in the lower stratosphere of the southern hemisphere: observations and modeling, J. Geophys. Res., 102, 3935–3949, 1997. 28878

Hanisco, T. F., Lanzendorf, E. J., Wennberg, P. O., Perkins, K. K., Stimpfle, R. M., Voss, P. B., Anderson, J. G., Cohen, R. C., Fahey, D. W., Gao, R. S., Hints, E. J., Salawitch, R. J., Margitan, J. J., McElroy, C. T., and Midwinter, C.: Sources, sinks, and the distribution of OH in the lower stratosphere, J. Phys. Chem. A, 105, 1543–1553, 2001. 28870, 28872, 28887

Hofmann, D., Barnes, J., O'Neill, M., Trudeau, M., and Neely, R.: Increase in background stratospheric aerosol observed with lidar at Mauna Loa Observatory and Boulder, Colorado, Geophys. Res. Lett., 36, L15808, doi:10.1029/2009GL039008, 2009. 28875, 28876

Jaeglé, L., Jacob, D. J., Brune, W. H., and Wennberg, P. O.: Chemistry of HO_x radicals in the upper troposphere, Atmos. Environ., 35, 469–489, 2001. 28871

Joiner, J., Schoeberl, M. R., Vasilkov, A. P., Oreopoulos, L., Platnick, S., Livesey, N. J., and Levelt, P. F.: Accurate satellite-derived estimates of the tropospheric ozone impact on the global radiation budget, Atmos. Chem. Phys., 9, 4447–4465, doi:10.5194/acp-9-4447-2009, 2009. 28873

Kley, D., Crutzen, P. J., Smit, H. G. J., Vömel, H., Oltmans, S. J., Grassl, H., and Ramanathan, V.: Observations of near-zero ozone concentrations over the convective Pacific: effects on air chemistry, Science, 274, 230–233, 1996. 28871

Krüger, K. and Quack, B.: Introduction to special issue: the *TransBrom Sonne* expedition in the tropical West Pacific, Atmos. Chem. Phys., 13, 9439–9446, doi:10.5194/acp-13-9439-2013, 2013. 28871

Krüger, K., Tegtmeier, S., and Rex, M.: Long-term climatology of air mass transport through the Tropical Tropopause Layer (TTL) during NH winter, Atmos. Chem. Phys., 8, 813–823, doi:10.5194/acp-8-813-2008, 2008. 28874

A Tropical West
Pacific OH minimum

M. Rex et al.

Title Page

Abstract

Introduction

Conclusions

References

Tables

Figures

◀

▶

◀

▶

Back

Close

Full Screen / Esc

Printer-friendly Version

Interactive Discussion



- Levy II, H.: Normal atmosphere: large radical and formaldehyde concentrations predicted, *Science*, 173, 141–143, 1971. 28871
- Liu, S. C., McFarland, M., Kley, D., Zafiriou, O., and Huebert, B.: Tropospheric NO_x and O₃ budgets in the Equatorial Pacific, *J. Geophys. Res.*, 88, 1360–1368, 1983. 28872
- 5 Madronich, S. and Flocke, S.: The role of solar radiation in atmospheric chemistry, in: *Handbook of Environmental Chemistry*, edited by: Boule, P., Springer-Verlag, Heidelberg, 1–26, 1999. 28880
- Manning, M. R., Lowe, D. C., Moss, R. C., Bodeker, G. E., and Allan, W.: Short-term variations in the oxidizing power of the atmosphere, *Nature*, 436, 1001–1004, 2005. 28870, 28871
- 10 Martinez-Aviles, M., Kreher, K., Johnston, P., Thomas, A., Hay, T., Schofield, R., and Kenntner, M.: Sources of halogen oxides along the coastline of New Zealand: a field measurement study, *Geophysical Research Abstracts*, 12, 673, 2010. 28875
- Montzka, S. A., Krol, M., Dlugokencky, E., Hall, B., Jöckel, P., and Lelieveld, J.: Small interannual variability of global atmospheric hydroxyl, *Science*, 331, 67–69, 2011. 28870
- 15 Newell, R. E. and Gould-Stewart, S.: A stratospheric fountain?, *J. Atmos. Sci.*, 38, 2789–2796, 1981. 28871
- Proffitt, M. H. and McLaughlin, R. J.: Fast-response dual-beam UV-absorption ozone photometer suitable for use on stratospheric balloons, *Rev. Sci. Instrum.*, 54, 1719–1728, 1983. 28878
- Pyle, J. A., Ashfold, M. J., Harris, N. R. P., Robinson, A. D., Warwick, N. J., Carver, G. D., Gostlow, B., O'Brien, L. M., Manning, A. J., Phang, S. M., Yong, S. E., Leong, K. P., Ung, E. H., and Ong, S.: Bromoform in the tropical boundary layer of the Maritime Continent during OP3, *Atmos. Chem. Phys.*, 11, 529–542, doi:10.5194/acp-11-529-2011, 2011. 28875
- 20 Quack, B., Atlas, E., Petrick, G., Stroud, V., Schauffler, S., and Wallace, D. W. R.: Oceanic bromoform sources for the tropical atmosphere, *Geophys. Res. Lett.*, 31, L23S05, doi:10.1029/2004GL020597, 2004. 28875
- Ridder, T., Gerbig, C., Notholt, J., Rex, M., Schrems, O., Warneke, T., and Zhang, L.: Shipborne FTIR measurements of CO and O₃ in the Western Pacific from 43° N to 35° S: an evaluation of the sources, *Atmos. Chem. Phys.*, 12, 815–828, doi:10.5194/acp-12-815-2012, 2012. 28873, 28878
- 30 Rohrer, F. and Berresheim, H.: Strong correlation between levels of tropospheric hydroxyl radicals and solar ultraviolet radiation, *Nature*, 442, 184–187, 2006. 28870
- Sander, S. P., Abbatt, J., Barker, J. R., Burkholder, J. B., Friedl, R. R., Golden, D. M., Huie, R. E., Kolb, C. E., Kurylo, M. J., Moortgat, G. K., Orkin, V. L., and Wine, P. H.: Chemical Kinetics and

A Tropical West
Pacific OH minimum

M. Rex et al.

Title Page

Abstract

Introduction

Conclusions

References

Tables

Figures

◀

▶

◀

▶

Back

Close

Full Screen / Esc

Printer-friendly Version

Interactive Discussion



- Photochemical Data for Use in Atmospheric Studies, Evaluation Number 17, JPL Publication 10-06, Jet Propulsion Laboratory, California Institute of Technology, Pasadena, 2011. 28880
- Scott, S. G., Bui, T. P., Chan, K. R., and Bowen, S. W.: The meteorological measurement system on the NASA ER-2 aircraft, *J. Atmos. Ocean. Tech.*, 7, 525–540, 1990. 28878
- 5 Solomon, S., Thompson, D. W. J., Portmann, R. W., Oltmans, S. J., and Thompson, A. M.: On the distribution and variability of ozone in the tropical upper troposphere: implications for tropical deep convection and chemical-dynamical coupling, *Geophys. Res. Lett.*, 32, L23813, doi:10.1029/2005GL024323, 2005. 28871
- Solomon, S., Daniel, J. S., Neely III, R. R., Vernier, J.-P., Dutton, E. G., and Thomason, L. W.:
10 The persistently variable “background” stratospheric aerosol layer and global climate change, *Science*, 333, 866–870, 2011. 28870, 28875
- Stevenson, D. S., Dentener, F. J., Schultz, M. G., Ellingsen, K., van Noije, T. P. C., Wild, O., Zeng, G., Amann, M., Atherton, C. S., Bell, N., Bergmann, D. J., Bey, I., Butler, T., Co-fala, J., Collins, W. J., Derwent, R. G., Doherty, R. M., Drevet, J., Eskes, H. J., Fiore, A. M.,
15 Gauss, M., Hauglustaine, D. A., Horowitz, L. W., Isaksen, I. S. A., Krol, M. C., Lamarque, J.-F., Lawrence, M. G., Montanaro, V., Müller, J.-F., Pitari, G., Prather, M. J., Pyle, J. A., Rast, S., Rodriguez, J. M., Savage, M. G. S. N. H., Shindell, D. T., Strahan, S. E., Sudo, K., and Szopa, S.: Multimodel ensemble simulations of present-day and near-future tropospheric ozone, *J. Geophys. Res.*, 111, D08301, doi:10.1029/2005JD006338, 2006. 28873
- 20 Thomason, L. and Peter, T.: Assessment of Stratospheric Aerosol Properties, SPARC Report No. 4, WMO/TD-No. 1295, 2006. 28875
- Vernier, J. P., Thomason, L. W., Pommereau, J.-P., Bourassa, A., Pelon, J., Garnier, A., Hauchecorne, A., Blanot, L., Trepte, C., Degenstein, D., and Vargas, F.: Major influence of tropical volcanic eruptions on the stratospheric aerosol layer during the last decade, *Geophys. Res. Lett.*, 38, L12807, doi:10.1029/2011GL047563, 2011. 28875, 28877
- 25 Vömel, H. and Diaz, K.: Ozone sonde cell current measurements and implications for observations of near-zero ozone concentrations in the tropical upper troposphere, *Atmos. Meas. Tech.*, 3, 495–505, doi:10.5194/amt-3-495-2010, 2010. 28878
- Weisenstein, D. K., Yue, G. K., Ko, M. K. W., Sze, N.-D., Rodriguez, J. M., and Scott, C. J.: A two-dimensional model of sulfur species and aerosols, *J. Geophys. Res.*, 102, 13019–13035,
30 1997. 28875
- Wennberg, P. O., Cohen, R. C., Hazen, N. L., Lapson, L. B., Allen, N. T., Hanisco, T. F., Oliver, J. F., Lanham, N. W., Demusz, J. N., and Anderson, J. G.: Aircraft-borne, laser-induced

fluorescence instrument for the in situ detection of hydroxyl and hydroperoxyl radicals, Rev. Sci. Instrum., 65, 1858–1876, 1994. 28878

WMO: World Meteorological Organization (WMO)/United Nations Environment Programme (UNEP), Scientific Assessment of Ozone Depletion: 2010, Global Ozone Research and Monitoring Project – Report No. 52, 2011. 28870, 28874

Wohlmann, I. and Rex, M.: The Lagrangian chemistry and transport model ATLAS: validation of advective transport and mixing, Geosci. Model Dev., 2, 153–173, doi:10.5194/gmd-2-153-2009, 2009. 28874, 28879

Wohlmann, I., Lehmann, R., and Rex, M.: The Lagrangian chemistry and transport model ATLAS: simulation and validation of stratospheric chemistry and ozone loss in the winter 1999/2000, Geosci. Model Dev., 3, 585–601, doi:10.5194/gmd-3-585-2010, 2010. 28874, 28879

Ziemke, J. R., Chandra, S., Duncan, B. N., Froidevaux, L., Bhartia, P. K., Levelt, P. F., and Waters, J. W.: Tropospheric ozone determined from Aura OMI and MLS: evaluation of measurements and comparison with the Global Modeling Initiative's Chemical Transport Model, J. Geophys. Res., 111, D19303, doi:10.1029/2006JD007089, 2006. 28873

ACPD

13, 28869–28893, 2013

A Tropical West Pacific OH minimum

M. Rex et al.

[Title Page](#)[Abstract](#)[Introduction](#)[Conclusions](#)[References](#)[Tables](#)[Figures](#)[I◀](#)[▶I](#)[◀](#)[▶](#)[Back](#)[Close](#)[Full Screen / Esc](#)[Printer-friendly Version](#)[Interactive Discussion](#)

A Tropical West Pacific OH minimum

M. Rex et al.

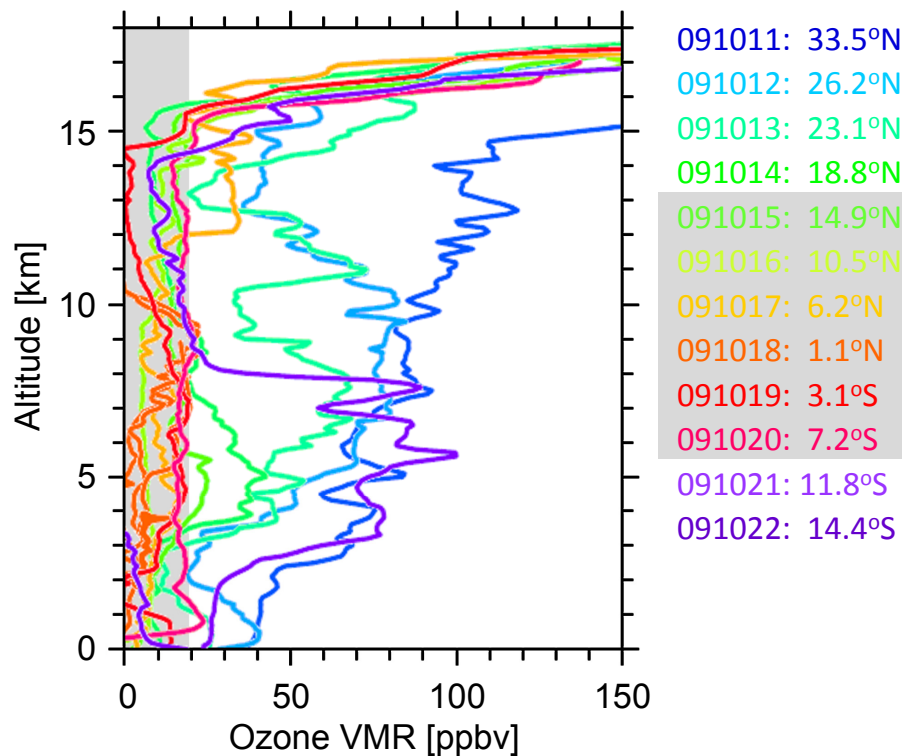


Fig. 1. West Pacific Tropospheric ozone from balloon sondes. Gray shading indicates detection limit (left) and soundings with ozone abundances mostly below the detection limit (right).

[Title Page](#)[Abstract](#)[Introduction](#)[Conclusions](#)[References](#)[Tables](#)[Figures](#)[◀](#)[▶](#)[◀](#)[▶](#)[Back](#)[Close](#)[Full Screen / Esc](#)[Printer-friendly Version](#)[Interactive Discussion](#)

A Tropical West Pacific OH minimum

M. Rex et al.

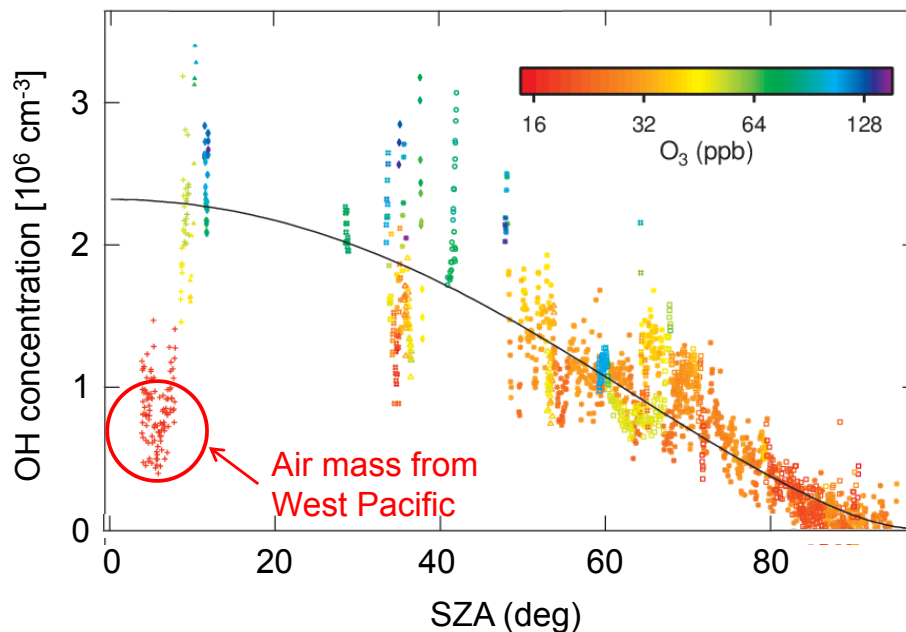


Fig. 2. OH vs. solar zenith angle (SZA) for measurements above 11 km during STRAT (10 s averages). Color indicates ozone mixing ratio. The black line represents the compact relation reported by Hanisco et al. (2001). The red circle indicates air masses from the West Pacific with extremely low ozone and OH. For these air masses NO is also extremely low (below $108 \text{ molecules cm}^{-3}$, not shown).

[Title Page](#)[Abstract](#)[Introduction](#)[Conclusions](#)[References](#)[Tables](#)[Figures](#)[◀](#)[▶](#)[◀](#)[▶](#)[Back](#)[Close](#)[Full Screen / Esc](#)[Printer-friendly Version](#)[Interactive Discussion](#)

A Tropical West Pacific OH minimum

M. Rex et al.

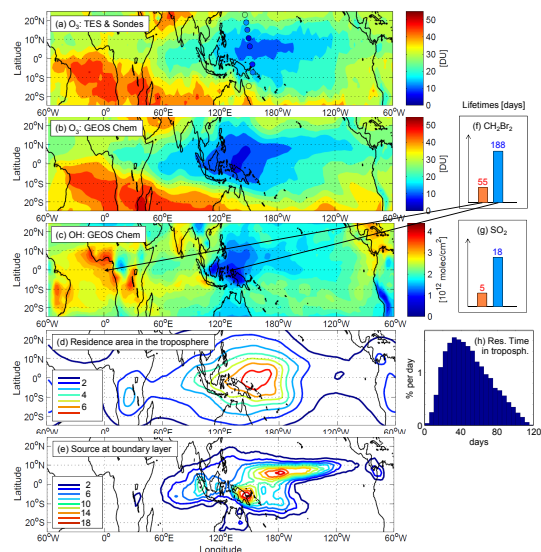


Fig. 3. Tropospheric ozone columns from **(a)** TES for October 2009 (results for 2005–2009 are similar, see Appendix), the sondes (dots, dates see Fig. 1), and **(b)** GEOS Chem (1–15 October 2009). **(c)** OH columns from GEOS-Chem (1–15 October 2009). **(d, e, h)** show ATLAS 4-months backtrajectory runs for air entering the stratosphere (starting 1 October). Average conditions for 2002–2011, individual results for 2009 are similar. **(d)** Density distribution function of the horizontal positions of the trajectories between the boundary layer and the LCPs. **(e)** Density distribution function of the horizontal positions of the last contact with the boundary layer. The values in **(d)** and **(e)** are normalized such that a horizontally uniform distribution corresponds to a value of 1 at every grid point. **(f–g)** Examples of gas phase lifetimes of relevant species in the mid-troposphere (500 hPa) at the equator for typical conditions over the Atlantic (0° E, orange) and for conditions in the OH minimum (130° E, blue). **(h)** Distribution of residence times between last contact with the boundary layer and the LCPs for air ascending into the stratosphere.

Title Page

Abstract

Introduction

Conclusions

References

Tables

Figures

◀

▶

◀

▶

Back

Close

Full Screen / Esc

Printer-friendly Version

Interactive Discussion



A Tropical West Pacific OH minimum

M. Rex et al.

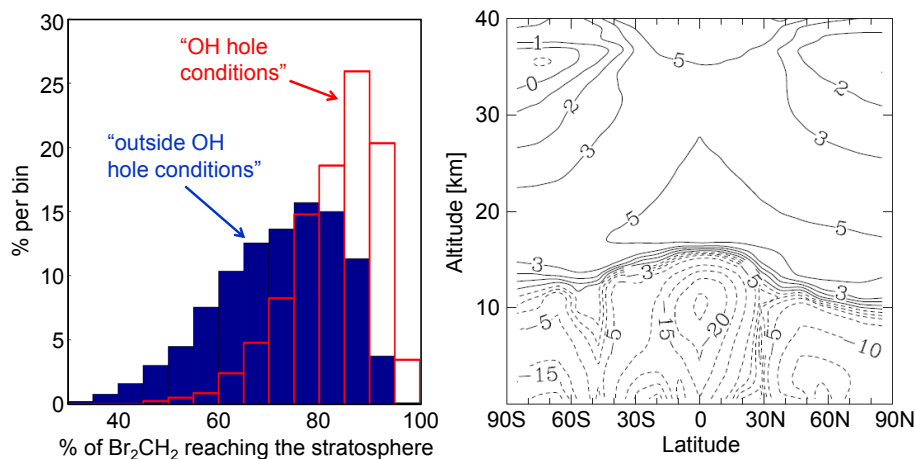


Fig. 4. (a) Distribution of the fraction of boundary layer CH_2Br_2 surviving the transport through the troposphere for “outside minimum” conditions (blue) and “OH minimum” conditions (red). (b) Percent difference in aerosol surface area densities between runs of the 2-D AER model for “OH minimum” and “outside minimum” conditions.

[Title Page](#)[Abstract](#)[Introduction](#)[Conclusions](#)[References](#)[Tables](#)[Figures](#)[◀](#)[▶](#)[◀](#)[▶](#)[Back](#)[Close](#)[Full Screen / Esc](#)[Printer-friendly Version](#)[Interactive Discussion](#)

A Tropical West Pacific OH minimum

M. Rex et al.

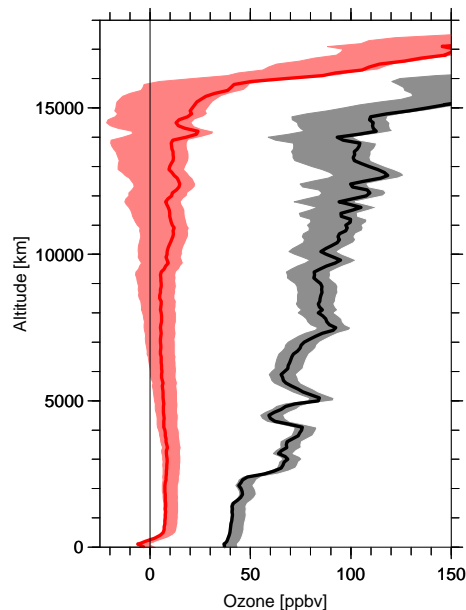


Fig. A1. Tropospheric ozone profiles at 33.5° N (black, 11 October) and at 10.5° N (red, 16 October). The shading illustrates the effect of different assumptions on the evolution of the background current during the sounding on the ozone mixing ratios calculated from the cell current. The lowest values (left hand edge of the shading) result from subtracting a constant background current, the highest values (right hand edge) from assuming that the background current drops to zero immediately after the launch, i.e., from not subtracting any background. The lines reflect the results from subtracting a pressure dependent background current (see text).

[Title Page](#)[Abstract](#)[Introduction](#)[Conclusions](#)[References](#)[Tables](#)[Figures](#)[◀](#)[▶](#)[◀](#)[▶](#)[Back](#)[Close](#)[Full Screen / Esc](#)[Printer-friendly Version](#)[Interactive Discussion](#)

A Tropical West Pacific OH minimum

M. Rex et al.

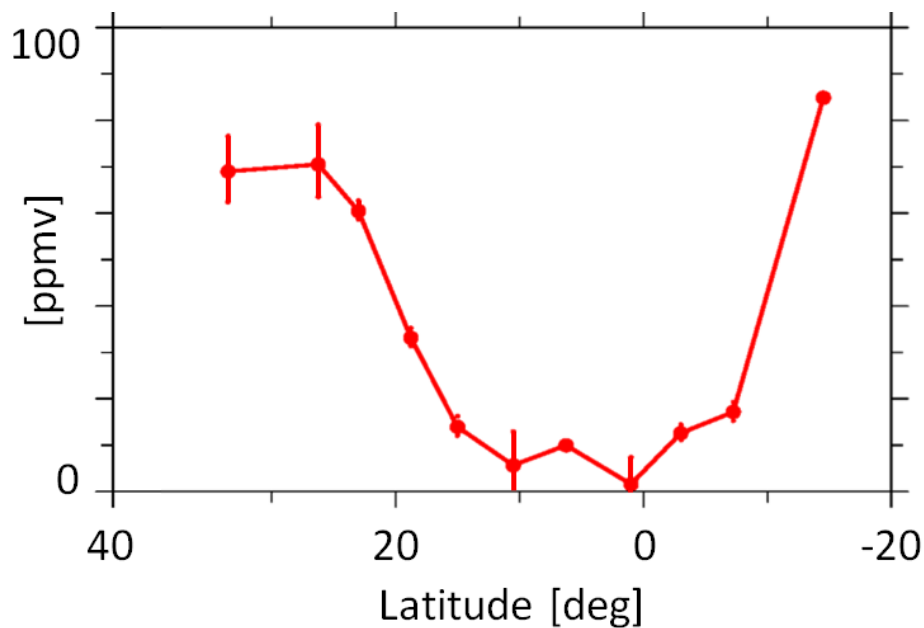


Fig. A2. Ozone mixing ratios measured by the sondes in the mid troposphere (500 hPa).

[Title Page](#)[Abstract](#)[Introduction](#)[Conclusions](#)[References](#)[Tables](#)[Figures](#)[◀](#)[▶](#)[◀](#)[▶](#)[Back](#)[Close](#)[Full Screen / Esc](#)[Printer-friendly Version](#)[Interactive Discussion](#)

A Tropical West Pacific OH minimum

M. Rex et al.

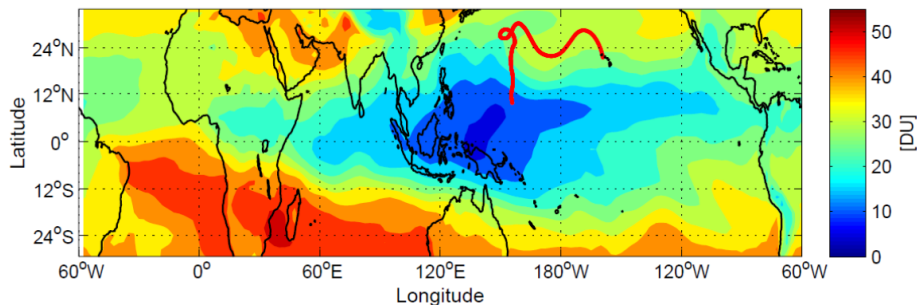


Fig. A3. 12 day back trajectory (red line) ending close to Hawaii of the air mass, which is indicated by the red circle in Fig. 2. Color indicates the tropospheric ozone column from Geos-Chem as in Fig. 3b.

[Title Page](#)[Abstract](#)[Introduction](#)[Conclusions](#)[References](#)[Tables](#)[Figures](#)[◀](#)[▶](#)[◀](#)[▶](#)[Back](#)[Close](#)[Full Screen / Esc](#)[Printer-friendly Version](#)[Interactive Discussion](#)

A Tropical West Pacific OH minimum

M. Rex et al.

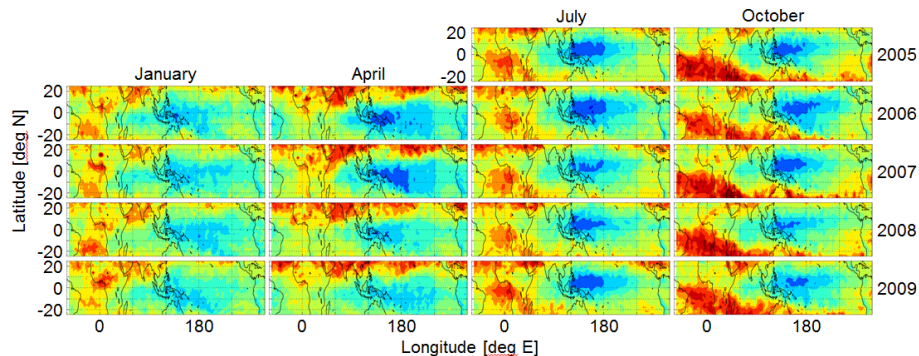


Fig. A4. Monthly mean tropospheric ozone columns from TES for January, April, July and October for the years 2005–2009.

[Title Page](#)[Abstract](#)[Introduction](#)[Conclusions](#)[References](#)[Tables](#)[Figures](#)[◀](#)[▶](#)[◀](#)[▶](#)[Back](#)[Close](#)[Full Screen / Esc](#)[Printer-friendly Version](#)[Interactive Discussion](#)